Conformations of Polymer Melts between Parallel Surfaces: Comparison of the Scheutjens–Fleer Lattice Theory with Monte Carlo Simulations†

Grant D. Smith

Eloret Institute, Sunnyvale, California 94087

Do Y. Yoon*

IBM Almaden Research Center, 650 Harry Road, San Jose, California 95120

Richard L. Jaffe

NASA Ames Research Center, Moffett Field, California 94035

Received June 15, 1992; Revised Manuscript Received August 31, 1992

ABSTRACT: Conformations of chains in polymer melts confined between parallel solid surfaces are examined by means of lattice Monte Carlo (MC) simulations and the Scheutjens–Fleer self-consistent-field (SCF) lattice theory for the purpose of comparing SCF predictions directly with simulation. The effects of surface–chain end interactions on conformational properties of the chains are investigated by considering nonadsorbing, weakly adsorbing, and strongly adsorbing chain ends. Quantitative agreement between MC simulations and SCF theory is found for segment and chain end density distributions and bond orientation profiles. The SCF theory reproduces major features of polymer conformations, as seen in the distributions of loops, tails, trains, and bridges, but quantitative comparisons show considerable differences which are attributed primarily to the reversible walk nature of the SCF theory. It was found that increasing the surface–chain end adsorption energy leads to the formation of more brushlike chain conformations, with more long tails and loops and fewer long train sequences.

Introduction

The use of polymer thin films in a variety of applications has inspired great interest in the influence of solid surfaces on polymer chain conformations, which play a critical role in determining system properties. The self-consistent-field (SCF) statistical lattice theory of Scheutjens and Fleer,[1,2] originally developed to describe polymer adsorption from solutions, has been applied extensively to a variety of polymer interfaces such as homopolymer/solid interfaces,[3] terminally attached polymer brushes,[4,5] interactions between adsorbed polymer layers,[6] block copolymer adsorption,[7] and surfactants at solid/liquid interfaces.[8] Direct comparison of the predictions of this SCF theory with simulations, however, appears to be limited to the case of terminally anchored polymer brushes,[4,5] where reasonable agreement between simulation and theory was obtained for segment density profiles. In this paper we utilize the Scheutjens–Fleer SCF theory to compute the conformational properties of polymer melts confined between parallel solid surfaces and compare results with Monte Carlo (MC) simulations based upon the configurational-bias self-avoiding random walk scheme of Rosenbluth and Rosenbluth.[9] In addition, the effects of surface–chain end adsorption energies on chain conformations are explored. A comparison of lattice theory predictions and MC simulations with atomistic simulations of polymethylene systems confined between parallel surfaces will be presented in a future paper.

Computational Methodology

Polymer System. The equilibrium conformations of a system of polymer chains confined between parallel solid surfaces were investigated via the Scheutjens–Fleer SCF theory and Monte Carlo simulations, as described below. Chains of length $n = 20$ segments confined to a simple cubic lattice of $m = 10$ layers, with layers 1 and 10 lying on the respective solid surfaces, were considered. Each layer of the Monte Carlo lattice was 20 units by 20 units with periodic boundary conditions. Although both the SCF theory and the Monte Carlo simulation method employed allow for complete occupancy of the lattice by chain segments, an occupancy fraction $\phi = 0.80$ was chosen in order to allow comparison of polymer segment density profiles. The nonoccupied sites were considered to interact with the polymer segments in an athermal fashion, although specific solvent–polymer interactions can be incorporated.[1,2] Nonend polymer segments were considered to have no net (relative to the empty sites) interaction with the surfaces. In order to investigate the effect of surface–chain end adsorption energies on chain conformations, four scenarios with respect to surface–chain end segment interactions were considered: no net interaction energy, one polymer end weakly adsorbing, both polymer ends weakly adsorbing, and both polymer ends strongly adsorbing. The differential adsorption energy $\chi_e = -\Delta E/kT$ for the surface–chain end interaction, where ΔE is the relative adsorption energy of a chain end segment on the surface relative to nonend segments, was 1.25 for weakly adsorbing ends and 4 for strongly adsorbing ends.

Scheutjens–Fleer SCF Theory. The primary advantage of the Scheutjens–Fleer theory over earlier approaches is that it avoids the assumption that chain segments located in any part of the chain contribute the same to the segment density at any distance from the surface. This allows for the inclusion of specific surface–chain end interactions. A brief description of the Scheutjens–Fleer SCF theory, along with the modifications incorporated to consider specific surface–chain end interactions, is presented here. For full details of the Scheutjens–Fleer SCF theory, readers are referred to the original papers.[1,2]

The Scheutjens–Fleer approach begins by considering the probability of finding a monomer in layer i of the lattice

† This work is dedicated to the memory of the late Jan Scheutjens.

0024-9297/92/2225-7011$03.00/0

relative to that in bulk solution, given by the free segment probability p_i. In the absence of specific segment–solvent and segment–surface interactions, p_i is given by

$$p_i = \frac{1 - \phi_i}{1 - \phi} \tag{1}$$

where the occupancy of each lattice layer i by polymer segments is given by ϕ_i. Obviously $\langle \phi_i \rangle = \phi$, where the average is taken over all lattice layers. Equation 1 represents an entropy factor accounting for the fact that a fraction of sites in each layer is occupied by segments.

A chain is constructed by joining monomer units numbered $s = 1, 2, ..., n$, where n is the length of the polymer chain. The probability that the end segment of a chain of r segments lies in layer i is given by $p(i,r)$. For a single segment, $p(i,1) = p_i$, the free segment probability. On a simple cubic lattice (coordination number of nearest neighbor sites = 6) the fraction of nearest neighbor sites lying in a given layer i is $\lambda_0 = {}^4/_6$ and the fraction lying in each of the adjoining layers is $\lambda_1 = {}^1/_6$. Hence a second monomer joined to the first monomer lying in layer i can lie in the same layer i or either of the adjacent layers $i + 1$ and $i - 1$ with probabilities given by $\lambda_0 p(i,1)p_i$, $\lambda_1 p(i,1)p_{i-1}$, and $\lambda_1 p(i,1)p_{i+1}$, respectively. The end segment probability $p(i,2)$, the probability that the end segment of a chain of 2 segments is in layer i, is therefore given by

$$p(i,2) = \{p(i-1,1)\lambda_1 + p(i,1)\lambda_0 + p(i+1,1)\lambda_1\}p_i \tag{2}$$

In the same manner, the end segment probabilities for an r-mer are given as

$$p(i,r) = \{p(i-1,r-1)\lambda_1 + p(i,r-1)\lambda_0 + p(i+1,r-1)\lambda_1\}p_i \tag{3}$$

Examination of eq 3 indicates that multiple occupancy of lattice sites (such as that arising from direct back-folding of chains) is not explicitly prohibited. Corrections of the random-walk model for excluded volume effects arise from the free segment probabilities (eq 1), and hence are mean-field in nature. Expressed in matrix formalism the end segment probabilities $\mathbf{p}(r)$ are given as

$$\mathbf{p}(r) = \mathbf{w}\mathbf{p}(r-1) \tag{4}$$

$$\mathbf{p}(r) = \mathbf{w}^{r-1}\mathbf{p}(1) \tag{5}$$

where $\mathbf{p}(r)$ has components $p(i,r)$ and $\mathbf{w}$ is an $m \times m$ tridiagonal transition probability matrix whose elements are given as

$$w_{ij} = \lambda_{j-i}p_i \tag{6}$$

where $\lambda_{j-i} = \lambda_1$ if $|i - j| = 1$, $\lambda_{j-i} = \lambda_0$ if $j = i$, and $\lambda_{j-i} = 0$ otherwise. Hence, $\mathbf{p}(r)$ can be generated by the matrix multiplication scheme from a set of p_i, which in turn is related to the segment density profile ϕ_i according to eq 1.

Critical to this derivation is the fact that any conformation of an n-mer with the sth segment in layer i can be described as consisting of two sequences, starting at each chain end, of length s and $n - s + 1$, respectively. That is, the probability of finding the sth segment of an n-mer in layer i, relative to bulk solution, $p(s,i;n)$, is equal to the joint probability that both chain sequences end in layer i, divided by p_i, or

$$p(s,i;n) = p(i,s)p(i,n-s+1)/p_i \tag{7}$$

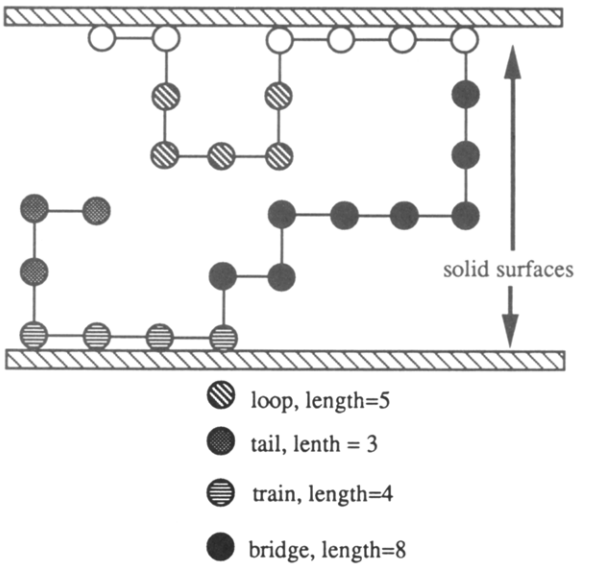

Figure 1. Schematic of adsorbed chains showing examples of loop, tail, train, and bridge sequences. All adsorbed segments form trains. Segments between trains form loops and bridges. Tails consists of segments between a free chain end and a train.

The segment density profile is then given by

$$\phi_i = \frac{\phi}{n}\frac{1}{p_i}\sum_{s=1}^{n} p(i,s)p(i,n-s+1) \tag{8}$$

where the sum is taken over each segment of the chain. An iterative approach[1] can be used to solve for ϕ_i. Starting with an initial guess for ϕ_i, eq 1 yields a set of p_i. From eq 8 and eq 1, new ϕ_i and p_i values are obtained. On convergence these p_i must yield through eq 8 the ϕ_i used to generate them.

To include specific surface–chain end interactions, the following extensions are introduced to the theory outlined above. We replace eq 4 by

$$\mathbf{p}(r) = \mathbf{w}(p(r)_i)\mathbf{p}(r-1) \tag{9}$$

The transition probability matrix becomes a function of r dependent "weighted" free segment probabilities $p(r)_i$. These probabilities are given by

$$p(r)_i = p_i \qquad 1 \le i \le m \qquad 1 \le r \le n$$

except

$$p(r)_i = p_i \exp(\chi_e(r,i)) \qquad i = 1, m \text{ and } r = 1, n \tag{10}$$

Here p_i are the free segment (unweighted) probabilities and $\chi_e(r,i)$ is the adsorption parameter for chain end r (1 or n) with surface i (1 or m).

The procedures described in ref 2 for calculation of the segment density and size distributions for loops, tails, and trains (see Figure 1 for definitions) were followed with the following modifications, which account for the presence of the second surface at layer m. In order to calculate distributions of loops, tails, and trains, end segment probabilities must be known for adsorbed r-mers (sequences with at least one segment in a surface layer) and free r-mers (sequences with no segments in a surface layer). For calculation of the end segment probabilities for free chains, $\mathbf{p}^f$ (eq 13, ref 2), the components of the transition probability matrix for free chains, $\mathbf{w}^f$ (eq 14, ref 2), are now given as

$$w^f_{ij} = \lambda_{j-i}p_i(1 - \delta_{1,i} - \delta_{m,i}) \tag{11}$$

Similarly, the components of $\mathbf{p}^f(1)$ (eq 15, ref 2), the free

segment probabilities for free chains, are given by

$$p^{f}(i,1) = p_i(1 - \delta_{1,i} - \delta_{m,i}) \tag{12}$$

For adsorbed chains, we consider each surface individually. Accordingly, the end segment probabilities for segments of length r adsorbed on layer 1, $\mathbf{p}_1^{a}(r)$, after eq A3 in ref 2, becomes

$$\mathbf{p}_1^{a}(r) = \mathbf{w}^{f}\mathbf{p}_1^{a}(r-1) + p(1,r)\Delta_1 \tag{13}$$

and for segments of length r adsorbed on layer m

$$\mathbf{p}_m^{a}(r) = \mathbf{w}^{f}\mathbf{p}_m^{a}(r-1) + p(m,r)\Delta_m \tag{14}$$

where Δ_1 is a column vector with the first component unity and the remaining zero and Δ_m is a column vector with the last component unity and the remaining zero. The first vectors $\mathbf{p}_1^{a}(1)$ and $\mathbf{p}_m^{a}(1)$ are

$$\mathbf{p}_1^{a}(1) = p(1,1)\Delta_1 \tag{15}$$

$$\mathbf{p}_m^{a}(1) = p(m,1)\Delta_m \tag{16}$$

End segment probabilities for tails of length r, $\mathbf{p}^{t}(r)$ (eq 43, ref 2), are now required for tails which end in layer 2 and layer $m - 1$. These are given as

$$\mathbf{p}_2^{t}(r) = (\mathbf{w}^{f})^{r-1}\mathbf{p}_2^{t}(1) \tag{17}$$

$$\mathbf{p}_{m-1}^{t}(r) = (\mathbf{w}^{f})^{r-1}\mathbf{p}_{m-1}^{t}(1) \tag{18}$$

respectively, where the components of $\mathbf{p}_2^{t}(1)$ and $\mathbf{p}_{m-1}^{t}(1)$ are

$$p_2^{t}(i,1) = p_2\delta_{2,i} \tag{19}$$

$$p_{m-1}^{t}(i,1) = p_{m-1}\delta_{m-1,i} \tag{20}$$

Expressions for the segment density and size distributions for loops and tails, as given in ref 2, which contain components of the end segment probabilities $\mathbf{p}^{a}$ and $\mathbf{p}^{t}$, now becomes expressions containing corresponding components of $\mathbf{p}_1^{a}$, $\mathbf{p}_m^{a}$, $\mathbf{p}_2^{t}$, and $\mathbf{p}_{m-1}^{t}$. Determination of the appropriate form of these expressions proceeds in a straightforward manner from the definitions given above and the corresponding expressions given in ref 2 for a single surface. For loops (eqs 23, 30, and 46 in ref 2), terms include products of end segment probabilities for two adsorbed chain segments. Bridges (see Figure 1 for definition) between the surfaces, which are a special case of loops, can be considered explicitly by separation of the cross-terms (i.e., terms containing products of end segment probabilities for chain segments adsorbed on different surfaces) from the complete expressions for loops.

Configurational-Bias Monte Carlo Simulations. The main advantage of Monte Carlo simulations over the Scheutjens–Fleer SCF theory is in the elimination of mean-field approximations for energies of mixing and excluded volume effects. The primary disadvantage is computational requirements, MC simulations being roughly 3 orders of magnitude more expensive in CPU time. Monte Carlo simulation procedures sample the conformational phase space of an ensemble of chains by changing chain conformations according to algorithms which yield configurations of the system with a probability as given by the partition function of the ensemble. For our MC simulations we utilize the Rosenbluth and Rosenbluth algorithm,[9] as implemented by Siepmann and Frenkel in their configurational-bias Monte Carlo scheme,[10] in our MC simulations. For a single chain on a 2-d lattice the algorithm is illustrated in Figure 2. After a chain end is chosen at random, a random number n_p of segments is "peeled" from the chain, where $1 \le n_p < n$. In Figure 2, $n_p = 2$. The first segment not peeled becomes the growing chain end. The chain is regrown in a sequential, segmental fashion in a trial configuration, with the last replaced segment becoming the growing chain end. The placement of a segment j (1 to n_p) is randomly selected among the $i = 1$ to z nearest neighbor lattice sites of the growing chain end according to

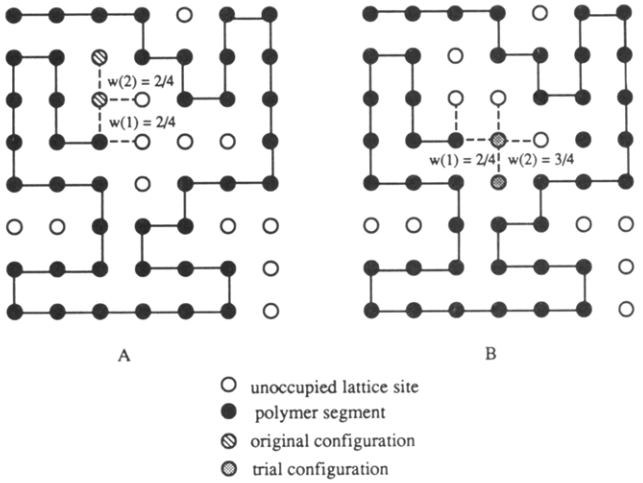

Figure 2. Example application of the configurational-bias Monte Carlo scheme. Shown is a single chain on a 2-D square lattice, with $z = 4$. In this example, two segments are peeled from a chain end and replaced. (A) shows the chain regrown in the original configuration. From eqs 23 and 24, $W_{original} = (2/4)(2/4) = 4/16$. (B) shows a trial configuration, where the segments have been placed randomly according to eq 23, which yields $P(1)_i = 1/2$, $i = 1, 2$ for the first segment and $P(2)_i = 1/3$, $i = 1, 3$ for the second, where only unoccupied sites are considered, occupied sites having zero weight. Here, $W_{trial} = (2/4)(3/4) = 6/16$. As $W_{trial}/W_{original} > 1$, the new configuration is accepted.

$$P(j)_i = B(j)_i / \sum_{k=1}^{z} B(j)_k \tag{21}$$

where $P(j)_i$ is the probability of placing segment j in the ith site. The $B(j)_i$ are the Boltzmann weights associated with placing segment j in each of the z nearest neighbor lattice sites of the growing chain end, which, when specific surface–chain end interactions are considered are given by

$$B(j)_i = 0 \quad \text{if the } i\text{th site is occupied}$$

otherwise

$$B(j)_i = \exp[\delta_{s,1}\delta_{d,1}\chi_e(1,1) + \delta_{s,1}\delta_{d,m}\chi_e(1,m) + \delta_{s,n}\delta_{d,1}\chi_e(n,1) + \delta_{s,n}\delta_{d,m}\chi_e(n,m)] \tag{22}$$

where s is the positional index (1 to n) of the segment j along the chain and d is the index of the lattice layer (1 to m) containing the ith nearest neighbor site. Hence eq 22 yields unity unless a chain end segment is being placed in a surface layer or a segment is being placed in an occupied site. The procedure is illustrated in Figure 2B. The placement of the segment is "biased" in that only unoccupied sites are considered for placement (occupied sites having zero probability), and these according to their Boltzmann weights. A Rosenbluth weight associated with

each replaced segment j is calculated according to the relationship

$$w(j) = \frac{\sum_{i=1}^{z} B(j)_i}{z} \tag{23}$$

where the sum is over the z nearest neighbor lattice sites of the growing chain end. When all peeled segments have been replaced, the Rosenbluth weight for the trial configuration is given by

$$W_{\text{trial}} = \prod_{j=1}^{n_p} w_j \tag{24}$$

In a similar fashion, the segments are replaced in their original configuration (Figure 2A) and the associated Rosenbluth weight W_{original} is determined. The Rosenbluth weights of each configuration account for the fact that only unoccupied sites, weighted according to their Boltzmann weights, were considered in regrowing the chains. The acceptance probability p_a for the trial configuration is given by

$$p_a = W_{\text{trial}}/W_{\text{original}} \tag{25}$$

When p_a is greater than a randomly generated number lying between 0 and 1, the trial configuration is accepted; otherwise, the original configuration is recounted. A series of configurational-biased moves, accepted according to eq 25, will sample the conformational phase space of the system as desired by yielding configurations with the correct probability. The primary advantage of the configurational-bias scheme is that disallowed trial conformations (those with multiple occupancy of lattice sites) are excluded from consideration by biasing segment placement to empty lattice sites on a segment by segment basis. This allows long chain sequences to be regrown with a reasonable probability for acceptance.

For our multichain system a few modifications were introduced in order to allow consideration of a densely occupied lattice. In our implementation a chain end is chosen at random. A search of the lattice is then performed along an axial direction chosen at random until another chain is encountered. An end of this second chain is then chosen at random. A random (but equal) number of segments is then peeled from each chain beginning at the chosen ends. The chains are regrown as described above, a segment at a time, alternating between chains. Each Monte Carlo run is the average of two runs of 50 million attempted moves each.

Results and Discussion

Density Profiles. The effects of the solid surfaces and chain end–surface interactions for weakly adsorbing ends on segment density and chain end density profiles are shown in Figures 3 and 4. Figure 3 shows a depletion of polymer segments on the surfaces. This effect is purely entropic, arising from restrictions imposed by the solid surfaces on chain conformations, and persists even when attractive surface–chain end interactions are included. Excellent agreement between SCF theory and MC simulation is indicated for all cases. Figure 4 indicates a slight entropy-driven increase in chain end density at the surfaces for the case of neutral chain ends. The density of chain ends at the surfaces increases dramatically when attractive interactions are included. Agreement between SCF theory and MC simulation is again quite good.

Bond Orientation Correlation. Bond orientation correlation is an indication of the degree of layering

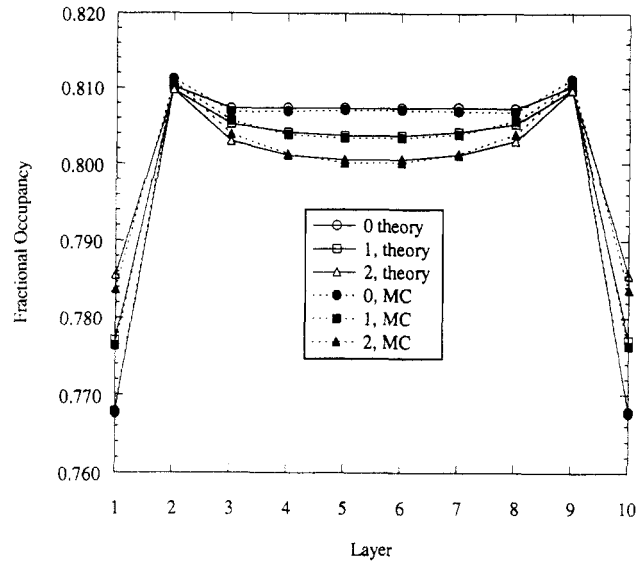

Figure 3. Segment density profiles. The fractional occupancy of lattice sites by polymer segments in each layer is shown. Theory indicates calculations according to the Scheutjens–Fleer theory. MC indicates the configurational-bias Monte Carlo results. Numbers in the legend indicate the number of chain ends per chain with net surface attraction $\chi_e = -\Delta E/kT$. For all cases illustrated $n = 20$, $m = 10$, $\phi = 0.80$, and $\chi_e = 1.25$.

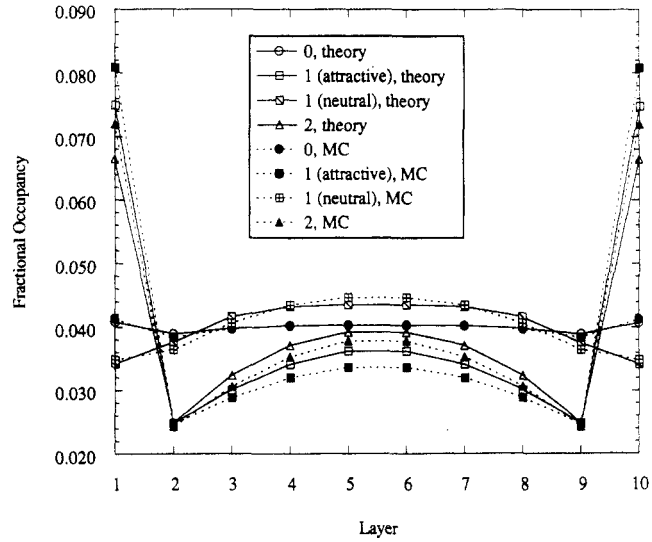

Figure 4. Density profiles for chain ends. Theory is the Scheutjens–Fleer SCF theory. MC is Monte Carlo simulations. Integers indicate the number of weakly adsorbing ends. For chains with one adsorbing end, distributions for both the adsorbing end and neutral end are shown. For cases with zero adsorbing and two adsorbing ends, fractional occupancy refers to a single end (multiply by 2 to obtain the total chain end occupancy).

imposed on the system by the solid surfaces. Expressed as a function of the layer index i, bond orientation correlation S_i is expressed as

$$S_i = \frac{1}{2}(3\langle\cos^2\theta\rangle_i - 1) \tag{26}$$

The average is taken over all bonds lying within, entering, or leaving layer i. Each bond forms an angle θ with an axis perpendicular to the layers. A value $S_i = 1$ indicates complete alignment perpendicular to the surfaces within layer i, while a value $S_i = -1/2$ indicates parallel alignment. Table I gives S_i as a function of layer index and number of weakly adsorbing chain ends. Significant orientation parallel to the surface exists only in the surface layers. Including weakly adsorbing chain ends has little influence

Table I
Bond Orientation Profiles

	number of weakly adsorbing ends					
	zero		one		two	
layer	theory	MC	theory	MC	theory	MC
1	−0.217 69	−0.214 89	−0.211 27	−0.212 55	−0.203 56	−0.200 50
2	0.013 80	0.015 51	0.016 62	0.018 82	0.020 27	0.026 64
3	−0.000 93	0.005 17	0.001 44	0.007 12	0.002 16	0.010 64
4	0.000 10	0.004 26	0.000 73	0.002 26	0.000 50	0.004 68
5	0.000 02	0.003 28	0.000 20	−0.001 34	0.000 25	0.000 12

on the degree of bond orientation correlation or the persistence of orientation from the surface. Excellent agreement between theory and simulation can been seen.

Chain Conformations. The effects of the surfaces and surface–chain end interactions on conformational properties of the chains can be investigated by determining the fraction of adsorbed chains (chains with any segment in a surface layer) and how segments of adsorbed chains are divided into loops, tails, trains, and bridges. These conformational features are illustrated in Figure 1. As seen in Table II, both theory and simulation indicate an increase in the fraction of adsorbed chains with the number of weakly adsorbing chain ends. However, the fraction of adsorbed chains is underestimated by the theory. This discrepancy is a result of the mean-field approximation inherent in the theory, which results in reversible random-walk (RW) type statistics with direct back-folding of chains. MC chains, following self-avoiding-walk (SAW) statistics with direct back-folding disallowed, exhibit a smaller number of adsorbed segments per adsorbed chain (see discussion on "trains" below), resulting in an increase in the number of chains encountering a surface.

Table II also shows the fraction of segments within adsorbed chains forming loops, tails, trains, and bridges and their weight-average sizes. Figures 5–8 show the fraction of segments *within adsorbed chains* forming loops, trains, tails, and bridges, respectively, of different sizes for weakly adsorbing ends. The average length of loops increases considerably as the number of attractive ends increases, as indicated in Table II. A similar effect is seen for tails. These effects are due to the higher density of chain ends on the surfaces for chains with attractive ends. As the density of chain ends (and segments near chain ends) on the surfaces increases, segments away from the ends are forced into loops (including bridges) and tails. These effects are also reflected in the loop and tail size distributions (Figures 5 and 6) which show an interesting increase in probability for longer loop and tail lengths for chains with attractive ends relative to nonattractive chains. In the limit of complete occupation of the surfaces by chain ends, all loops and tails would be of the maximum possible length.

In general good qualitative agreement between theory and simulation is seen for loops and tails, with gross differences being due to the RW nature of the SCF theory. For example, the SCF theory allows loops of length 1, which cannot occur in SAW chains. The odd–even effect seen in the loop size distributions (Figure 5) from simulation is not seen in the SCF distribution because of the additional loop configurations available to the RW chains.

Both theory and simulation show a decrease in the fraction of segments involved in trains and the average size of trains as the number of attractive ends increases (Table II). Both theory and simulation also reveal a systematic decrease in the probability of longer trains with increasing number of attractive ends, as shown in Figure 7. In the limit of complete occupation of the surfaces by chain ends, all trains would be of length 1. Although qualitative agreement for trains is indicated between SCF theory and MC simulations, deviation between theory and simulation is more serious for trains than for loops and tails. The SCF theory seriously overpredicts the probability of longer trains. The 2-D nature of train conformations exacerbates differences between RW and SAW chains. The effect is due mainly to the back-folding nature of the RW chains, not to longer range excluded volume effects. The fact that the theory reasonably predicts the decrease in the probability of long trains with increasing density of chain ends on the surface indicates that the Bragg–Williams approximation accounts adequately for long-range excluded volume effects. The theory also predicts a significantly higher probability for trains of length 1 (see Figure 7) than is seen from simulation. For SAW chains, trains of length 1 can form only at the chain ends, whereas for RW chains they can form anywhere along the chains.

An interesting feature indicated by both theory and MC is the abrupt increase in probability for a train of length n over a train of length $n - 1$, where n is the total number of segments in a chain, as seen in Figure 7. It is simple to show that for a RW on a cubic lattice the number of conformations available to a completely adsorbed chain is greater than that to a chain with a single end unit not adsorbed. The SAW nature of the MC simulation reduces this effect. Similar results have also been seen in off-lattice stochastic dynamics simulation of alkane melts between parallel surfaces,[11] where the effect is much more marked due to the greater persistence length (in terms of bonds or segments) of the alkanes relative to the lattice chains.

Next, we consider bridges. Because the separation of the surfaces is greater than the rms end-to-end distance of the chains, bridges are statistically rare, as indicated in Table II. The extended nature of the SAW chains relative to the RW chains results in a much higher fraction of segments forming bridges in the simulations than predicted by the SCF theory, as indicated in Table II and Figure 8. An interesting feature is the dramatic increase in the fraction of segments in adsorbed chains forming bridges with the number of adsorbing chain ends, seen in Table II. A more detailed discussion of bridges is reserved for a future publication, where we will consider cases with chains of rms dimension comparable to the surface separation, resulting in significant bridge formation.

Chain End Adsorption Energy. The distributions of segments for adsorbed chains between tails, trains, and loops, as determined from SCF theory and MC simulations, for chains with two strongly ($\chi_e = 4$) adsorbing ends, are shown in Figure 9. Trends indicated in Figures 5–7 for the case of weakly adsorbing chain ends are accentuated by increasing the adsorption energy. As the adsorption energy is increased, the surface is occupied to a greater extent by chain ends and segments near chain ends. The fraction of surface sites occupied by chain ends for chains with both ends adsorbing is (SCF theory, MC) 0.082, 0.082 for zero adsorption energy, 0.133, 0.144 for weakly adsorbing ends, and 0.306, 0.282 for strongly adsorbing ends. As a result chains form more brushlike conformations, with an increased frequency of long loops and tails. The effect is particularly dramatic for loops, where the peak in the segmental distribution has moved from short to very long loops. Long trains and short tails have essentially disappeared. The fraction of segments participating in bridges also increased dramatically (0.010 SCF, 0.049 MC; compare with Table II). Comparison of SCF theory with

Table II
Conformational Properties

property	number of weakly adsorbing ends: zero theory	zero MC	one theory	one MC	two theory	two MC
fraction of chains						
free	0.4794	0.4135	0.4373	0.3651	0.4129	0.3358
adsorbed	0.5206	0.5865	0.5627	0.6349	0.5871	0.6642
fraction of segments in adsorbed chains forming						
loops	0.1268	0.1230	0.1448	0.1421	0.1797	0.1825
tails	0.5044	0.5487	0.5094	0.5502	0.4850	0.5177
trains	0.3688	0.3272	0.3453	0.3055	0.3343	0.2956
bridges	0.0001	0.0010	0.0004	0.0021	0.0009	0.0043
wt av size of						
loops	6.408	6.986	7.216	7.878	8.289	8.921
tails	12.058	12.073	13.447	13.524	14.376	14.433
trains	7.312	6.264	6.866	5.814	6.514	5.447
bridges	15.115	14.988	15.440	15.476	15.769	15.578

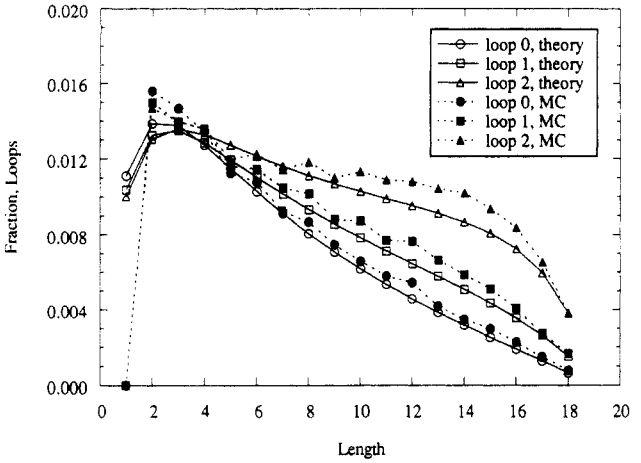

Figure 5. Fraction of segments within adsorbed chains forming loops of different sizes. Theory is the Scheutjens–Fleer SCF theory. MC is Monte Carlo simulations. Integers indicate the number of weakly adsorbing ends.

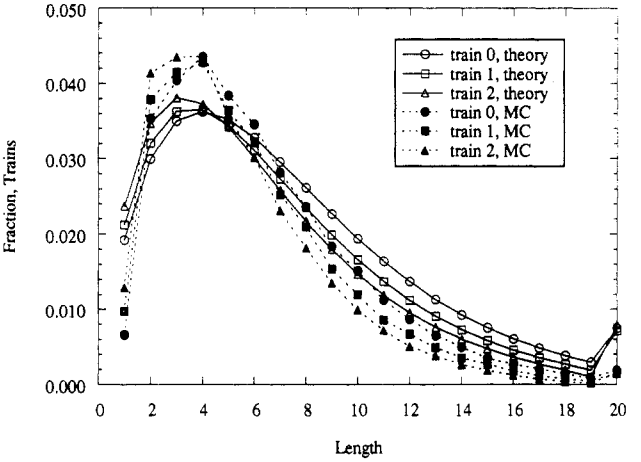

Figure 7. Fraction of segments within adsorbed chains forming trains of different sizes. Theory is the Scheutjens–Fleer SCF theory. MC is Monte Carlo simulations. Integers indicate the number of weakly adsorbing ends.

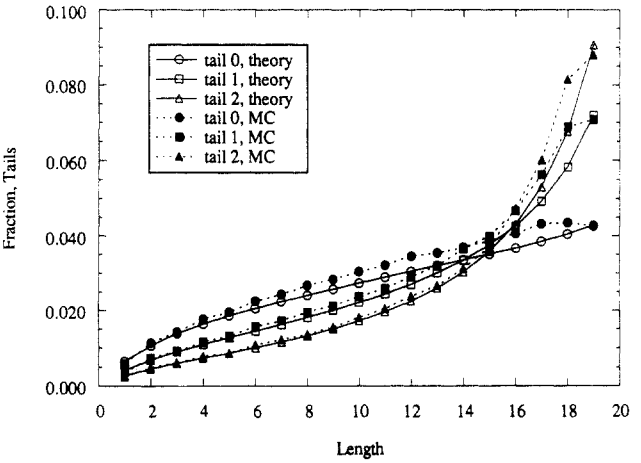

Figure 6. Fraction of segments within adsorbed chains forming tails of different sizes. Theory is the Scheutjens–Fleer SCF theory. MC is Monte Carlo simulations. Integers indicate the number of weakly adsorbing ends.

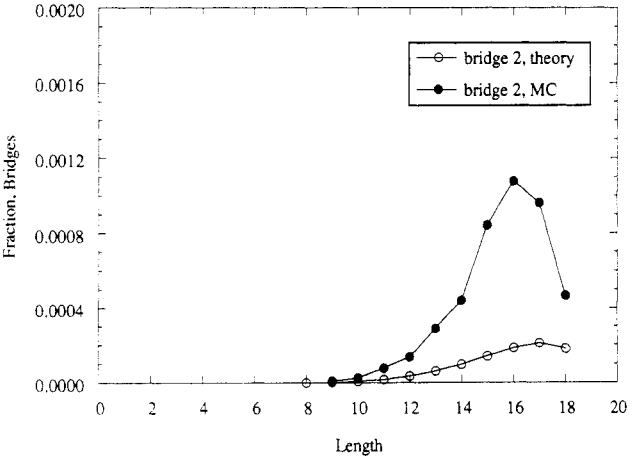

Figure 8. Fraction of segments within adsorbed chains forming bridges of different sizes. Theory is the Scheutjens–Fleer SCF theory. MC is Monte Carlo simulations. Integers indicate the number of weakly adsorbing ends.

MC again indicates good qualitative agreement, with best agreement for tails and greatest deviation in long trains.

Conclusions

The Scheutjens–Fleer SCF theory adequately reproduces segment density profiles and chain end density profiles for the polymer melts confined between two solid surfaces for the three different cases of surface–chain end interactions considered in the paper. Bond orientational distribution is also well represented by the theory. Chain conformations are less accurately represented, with the reversible (back-folding) nature of the RW chains, not the mean-field treatment of longer range excluded volume effects, being the primary shortcoming of the theory. Additional evidence supporting this conclusion is found in the work of Leermakers and co-workers.[12] In their work the Scheutjens–Fleer SCF theory was extended to exclude direct back-folding (thereby forming semi-SAW chains)

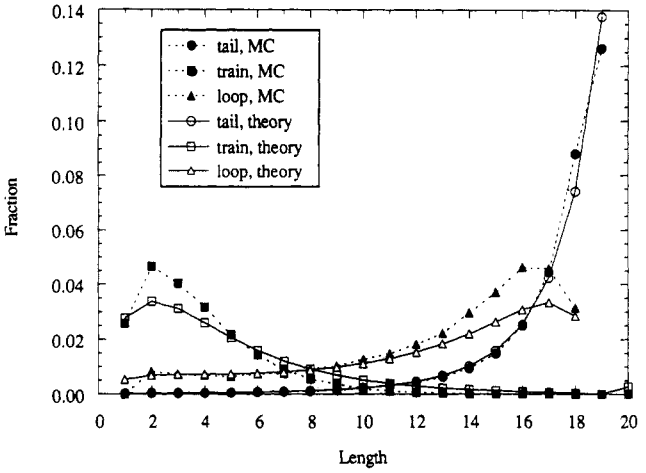

Figure 9. Fraction of segments within adsorbed chains forming tails, trains, and loops of different sizes for chains with strongly adsorbing ($\chi_e = 4.00$) ends. Theory is the Scheutjens–Fleer SCF theory. MC is Monte Carlo simulations.

in addressing the conformations of chains in the interlamellar noncrystalline region of a semicrystalline polymer. Differences found in the distributions of loops and bridges between RW SCF and semi-SAW SCF calculations qualitatively agree with the differences we found between SCF and MC calculations. A direct comparison of semi-SAW SCF theory with MC simulations would be quite interesting. We find the discrepancies are magnified for conformations confined to a surface layer (i.e., trains) and in extended conformations (i.e., bridges) and are least serious for the least confined conformations (i.e., tails). Despite these shortcomings, major conformational features are reproduced well qualitatively by the SCF theory. The effects of surface–chain end adsorption are also well reproduced by the theory, where it is found that greater adsorption energies lead to dramatic increases in brushlike conformations (long loops and tails) and a corresponding decrease in long adsorbed sequences (trains).

References and Notes

(1) Scheutjens, J. M. H. M.; Fleer, G. J. *J. Phys. Chem.* **1979**, *83*, 193.
(2) Scheutjens, J. M. H. M.; Fleer, G. J. *J. Phys. Chem.* **1980**, *84*, 178.
(3) Theodorou, D. N. *Macromolecules* **1988**, *21*, 1400.
(4) Cosgrove, T.; Health, T.; van Lent, B.; Leermakers, F.; Scheutjens, J. *Macromolecules* **1987**, *20*, 1692.
(5) Chakrabarti, A.; Toral, R. *Macromolecules* **1990**, *23*, 2016.
(6) Scheutjens, J. M. H. M.; Fleer, G. J. *Macromolecules* **1985**, *18*, 1882.
(7) Evers, O. A.; Scheutjens, J. M. H. M.; Fleer, G. J. *J. Chem. Soc., Faraday Trans.* **1990**, *86*, 1333.
(8) Fleer, G. J. *Colloids Surf.* **1989**, *35*, 151.
(9) Rosenbluth, M. N.; Rosenbluth, A. W. *J. Chem. Phys.* **1955**, *23*, 356.
(10) Siepmann, J. I.; Frenkel, D. *Mol. Phys.* **1992**, *75*, 59.
(11) Matsuda, T.; Winkler, R. G.; Yoon, D. Y. *Polym. Prepr. (Am. Chem. Soc., Div. Polym. Chem.)* **1992**, *33*, 687.
(12) Leermakers, F. A. M.; Scheutjens, J. M. H. M.; Gaylord, R. J. *Polymer* **1984**, *25*, 1577.